Automatic Location of Phase Singularities in Cardiac Spiralwave Reentry Simulation

Yinglan Gong[1], Dongdong Deng[1], Yu Zhang[2], Ling Xia[1]

[1] Zhejiang University, Hangzhou, China
[2] Patent Examination Cooperation Center of SIPO, Beijing, 100086, China

Abstract

Cardiac arrhythmias can be sustained by a number of reentry waves, which continuously propagates into recovered tissue and rotates around a central core. In experiments, the reentry waves are usually recorded in two dimensions and the phase singularity (PS) is used to quantitatively study the complex spatiotemporal patterns of fibrillation. In this paper, we propose an automatic method to identify the PS in two dimensions. With the cardiac reentry simulations, the efficiency, accuracy and parameter sensitivity of the proposed method were studied and compared with two commonly used methods. The results showed that the proposed method is more time-saving and less parameter sensitive than the previous methods. Furthermore, the detecting progress of the proposed method is automatic and can accurately detect the PSs without changing any parameters for different heart cell models, which is especially important for 3D whole heart simulation, since a lot of different cell types exist in the heart.

1. Introduction

Heart excitation is initialized at sinoatrial node and propagated along the electrical conduction system. In the abnormal situations, if there exists an anatomical obstacle, for example, a reentry or spiral waves may be raised, and thus tachycardia or even fibrillation may be produced. Evidences have shown that the transition from tachycardia to fibrillation is a transition to spatiotemporal chaos, with similarities to the quasi-periodic transition to chaos seen in fluid turbulence. Spiral-wave reentry could be unstable, and spiral waves can break up to form multiple spiral waves, which are similar to wave fronts observed during cardiac fibrillation. Movement of multiple spiral waves and their cores (phase singularities, PSs) is very complex, and can only be explained and investigated by nonlinear dynamics and chaos theory. Spiral waves have been extensively studied for their importance in understanding atrial and ventricular fibrillations, they provide valuable insights into the initiation and maintenance of the reentry in the human heart (1-5). The spiral waves can be caused by anatomic reentry (6-8) or functional reentry (3-4, 9). In either cases, an action potential continuously propagates into recovered tissue and rotates around a central core of excitable but unexcited tissue (10-11), it can break down into multiple reentrant waves which may be the cause of atrial and ventricular fibrillations. To locate the core of multiple reentrant waves is necessary for understanding of the initiation, termination and interaction of spiral waves (12).

When a wavebreak occurs through the interaction of the wavefront with anatomical or functional obstacles, a phase singularity (PS) appears, which is defined as a point whose phase is undefined, but is surrounded by the whole range of phases from $-\pi$ to π (12). The identification of PS is essential for analyzing the mechanisms underlying fibrillation in experimental or numerical models.

Previous studies have been performed the location of a numerically simulated filament in various ways (13-16), and many researchers have proposed different approaches to identify the location of PS, in which two methods are often used, one by Fenton and Karma (13) and the other by Iyer and Gray (14). Many refined algorithms based on the second method have been developed.

In this study, we propose a refined method based on Iyer and Gray (14), and then used it to locate the phase singularities (PSs) for several reentrant wave cases. In addition, the proposed method is compared with the method by Fenton and Karma (13) in performances of efficiency, accuracy and parameter sensitivity.

2. Materials and methods

2.1. Computer simulation of cardiac excitation propagation

The monodomain model (17) was used to study the propagation of action potential (AP), it was expressed by

the following partial differential equation,

$$\frac{\partial V_m}{\partial t} = D\left(\frac{\partial^2 V_m}{\partial x^2} + \frac{\partial^2 V_m}{\partial y^2}\right) - \frac{I_{ion}}{C_m} \quad (1)$$

where V_m is the transmembrane voltage, D represents the diffusion coefficient, C_m is the membrane capacitance, and I_{ion} is the sum of ionic currents. In order to test our method for PS location, we used two cell models to represent the I_{ion}, one is the human atrial appendage cell model developed by Seemann et al (18) and another is atrial fibrillation-induced electrical remodeling (AFER) cell model (19).

2.2. Methods for tracing phase singularities

The proposed method is based on the spatial distribution of phase proposed by Iyer and Gray (12, 14). In computer simulation or experimental research, the AP of cardiac fibrillation is usually recorded at a constant time step Δt, which is discrete, therefore, the series AP of cardiac fibrillation can be represented as V(nΔt) (n = 0,1,2,3,…). The spatial distribution of transmembrane potentials is converted into the distribution of phase which can be calculated from the potential of V(nΔt) and V((nΔt+τ) (τ is often chosen as a value between 2ms to 25ms) (14, 20), then the phase can be expressed as

$$\theta(t) = \arctan 2[V(n\Delta t + \tau) - V_{ref,y}, V(n\Delta t) - V_{ref,x}] \quad (2)$$

where ($V_{ref,x}$,$V_{ref,y}$) is the original point which should be chosen carefully, the inappropriate selection will make the PSs located inaccurately, and even get the wrong results.

There are many methods have been developed to select $V_{ref,x}$ and $V_{ref,y}$ (14, 16, 21). Firstly, we randomly selected the AP distribution of cardiac fibrillation at time nΔt and nΔt+τ. Then the state space was constructed by plotting $V(n\Delta t)$ against $V(n\Delta t+\tau)$. After that, randomly selected several points from the state space and used the direct least-square method to fit these points to an ellipse form (16) , then the average value was chosen as $V_{ref,x}$ and $V_{ref,y}$.

Once the $V_{ref,x}$ and $V_{ref,y}$ were gotten, the AP was translated into the phase space $\theta(t)$ by Eq. (2), and the PSs can be computed as follows:

$$\oint_P \nabla\theta \bullet dr = \begin{cases} \pm 2\pi & \text{if P encloses a phase singularity;} \\ 0 & \text{otherwise.} \end{cases} \quad (3)$$

The line integral is taken over path r on a closed curve P, if the phase difference is equal to ±2π, the path encloses a PS. For discrete space, the line integral of Eq. (3) at point (x, y) can be calculated by the following convolution operation,

$$\oint_P \nabla\theta \bullet dr \propto \nabla_x \otimes k_y + \nabla_y \otimes k_x \quad (4)$$

where $k_x = \theta(x+1,y) - \theta(x,y)$, $k_y = \theta(x,y+1) - \theta(x,y)$ and $\nabla_x = \begin{pmatrix} 1 & -1 \\ 0 & 0 \end{pmatrix}$, $\nabla_y = \begin{pmatrix} -1 & 0 \\ 1 & 0 \end{pmatrix}$

The second method we used for PSs location was proposed by Fenton and Karma (13), it was defined as the intersection point of the lines V_m=V_{iso} and dV_m/dt=0, V_{iso} was a constant membrane potential which can be chosen arbitrarily, but different values would influence on the accuracy of tip tracing. In 2D simulation, the time and space was discrete, for the time discrete, we use t repents the current time, t+1 repents the next time, for the space discrete, the cardiac tissue was discrete as M×N points, and $V_{i,j}^t$ represents the potential of point (i, j) at time t, according to the reference (13), V_m=V_{iso} and dV_m/dt=0 can be rewritten as

$$(1-m)(1-n)V_{i,j}^t + m(1-n)V_{i+1,j}^t + mnV_{i+1,j+1}^t + (1-m)nV_{i,j+1}^t = V_{iso} \quad (5)$$

$$(1-m)(1-n)V_{i,j}^{t+1} + m(1-n)V_{i+1,j}^{t+1} + mnV_{i+1,j+1}^{t+1} + (1-m)nV_{i,j+1}^{t+1} = V_{iso} \quad (6)$$

If equations (5) and (6) have a solution with $0 \le m < 1$ and $0 \le n < 1$, there exits filament in the square. In our simulation, if point (i, j) satisfied the equation (5) and (6), we choose this point as the filament, the remaining points were detected in the same way.

The second method we used for PSs location was proposed by Fenton and Karma (13), it was defined as the intersection point of the lines Vm=Viso and dVm/dt=0, Viso was a constant membrane potential which can be chosen arbitrarily, but different values would influence on the accuracy of tip tracing.

3. Results

We used a cross-field protocol to initialize the reentry of cardiac excitation propagation. The size of square in our simulations was 400×400 and the spatial resolution was 0.1mm, the time step was 0.1ms. The first voltage stimulus was added at one edge of the square for 1ms with the strengthen 10mv, sometime later, another voltage stimulus was added at the half bottom of the square for 1ms with the strengthen 20mv. After a sufficient time, the spiral wave broke up into fibrillation.

We used two methods to detect the PSs in cardiac reentry simulation, one is our refined method based on the spatial distribution of phase proposed by Iyer and Gray (12, 14) (Method I hereafter), another is the method

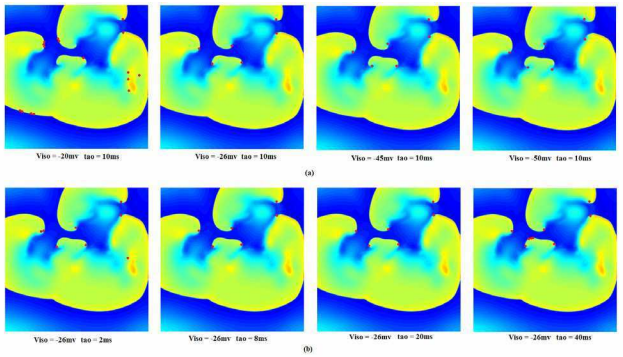

Figure 1. The PSs detecting using the using the Fenton and Karma method (13) at time 6500ms after the initiation of reentry. (a) The results of using different Viso and same time delay τ, (b) the results of using same Viso and different time delay.

proposed by Fenton and Karma (13) (Method II hereafter). The results have shown that both methods can identify the PSs, but they have different time-consuming, accuracy, adaptability and stability. In Method I, the most time consuming step is calculating the reference AP, in our simulation, it cost about 36 seconds on a personal computer with Intel(R) Core(TM) i7 CPU 920 @ 2.67GHz and 12 GB system memory, after the reference AP is obtained, it is used to calculate PSs of all images, and tracing one image cost about 0.05s. In Method II, in order to find PSs in one image, equations (5) and (6) must be calculated in each point throughout the image, since they are nonlinear equations, it is more time consuming, in our simulation, tracing one image need about 0.5s, furthermore, the more PSs in one image, the more time will be needed. So, in the viewpoint of time consuming, Method I is better than Method II.

For the method proposed by Fenton and Karma (13), we chose the value Viso from -10mv to -70mv and the step is 1mv, the value of time delay τ from 1ms to 40ms and the step is 1ms. Figure 1 showed the results of PSs location with different Viso and τ. Figure 1(a) showed the results that with the same time delay τ, but different Viso. We can see that the number of PSs was six, the value of Viso bigger than -26mv and smaller than -45mv can not accurately locate the PSs. If Viso was too small, the number of PSs is correct, but the location of PSs was not accurate. If Viso was too big, the additional points which were not PSs were detected, furthermore, some of the PSs were not detected. Figure 1(b) showed the results of using the same Viso and different time delay τ, when Viso was chosen as -26mv, the time delay τ varying from 8ms to 40ms can get good results.

The time delay τ has effect on the location of PSs. Therefore, in our simulation, we chose time delay τ from 2ms to 50ms, and the results were shown in figure 2. Figure 2(a) was the original AP distribution of fibrillation.

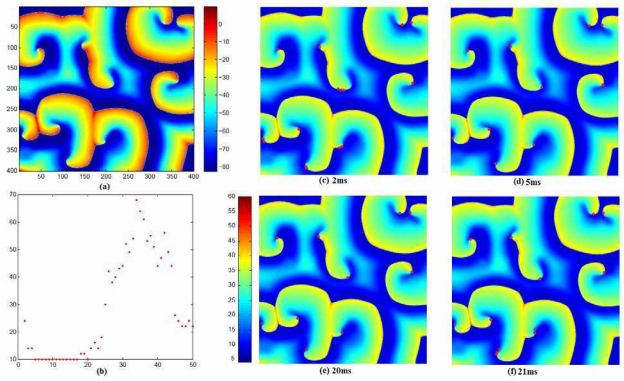

Figure 2. Phase distributions in different time. (a) The AP distribution at one time, (b) the number of PSs in different time delay, (c) to (f) showed the PSs locations and the AP distributions at different time of 2ms, 5ms, 20ms and 21ms.

Figure 2(b) displayed the detected PSs in each τ of figure 2 (a). When τ was within the range of 5ms to 20ms, the PSs can be detected accurately (see figure 2(d) and (e)), otherwise, some wrong PSs would be detected (see figure 2(c) and (f)).

4. Discussion and conclusions

In Method I, the simulation results show that our method is not parameter sensitive to the selection of time delay, it can varies from 5ms to 20ms freely. When we chose the same time delay (τ=10ms) in the two AP models used to form different fibrillations, the results showed that the PSs could be accurately detected.

In Method II, we must set Viso and τ to calculate the PSs, our simulation results show that the value selection of Viso and τ is important for the accuracy. Viso should not be too small or too big, -45mv ~ -26mv could get idea results. Furthermore, the time delay τ must be chosen carefully when changing Viso. In some cases, no matter what Viso and time delay τ were chosen, the PSs detection results were not satisfied.

For different cell models, Method I is robust and can accurately detect the PSs without need changing any parameters, but Method II has different results for different cell models. For atrial appendage cell model, Method II is not robust and cannot accurately detect the PSs in all images. For AFER cell model, Method II can accurately detect the PSs in most of the images, but in some images the parameters must be changed so as to correctly detect the PSs.

Human heart has different cell types. Since Method II is sensitive to parameter selection, and for different cell types it needs to change the Viso or time dalay τ, if it is used in the 3D human atrial fibrillation simulation, Method II may be not suitable. In the near future, we will use our method to detect the PSs in 3D human atrial

fibrillation simulation.

In all, we have used an anatomically detailed atrial model containing major conduction bundles and fiber orientation to simulate AF. The simulation results showed that re-entry waves could be initiated using the controlled state cell models if the electrophysiological heterogeneity exists in atria tissue, the APD restitution does not play the main role in the areas where the tissue heterogeneities are high. Fiber orientation is very important in sustaining of re-entry waves in the ectopic focus stimulation.

Acknowledgements

This project is supported by the 973 National Basic Research & Development Program of China (2007CB512100).

References

[1] Gong YF, Xie F, Stein KM, Garfinkel A, Culianu CA, Lerman BB, et al. Mechanism underlying initiation of paroxysmal atrial flutter/atrial fibrillation by ectopic foci - A simulation study. Circulation. 2007 Apr 24;115(16):2094-102.

[2] Bernus O, Verschelde H, Panfilov AV. Reentry in an anatomical model of the human ventricles. Int J Bifurcat Chaos. 2003 Dec;13(12):3693-702.

[3] Jacquemet V, Virag N, Kappenberger L. Wavelength and vulnerability to atrial fibrillation: Insights from a computer model of human atria. Europace. 2005 Sep;7:S83-S92.

[4] Ten Tusscher KHWJ, Hren R, Panfilov AV. Organization of ventricular fibrillation in the human heart. Circ Res. 2007 Jun 22;100(12):E87-E101.

[5] Virag N, Jacquemet V, Henriquez CS, Zozor S, Blanc O, Vesin JM, et al. Study of atrial arrhythmias in a computer model based on magnetic resonance images of human atria. Chaos. 2002 Sep;12(3):754-63.

[6] Aslanidi OV, Boyett MR, Dobrzynski H, Li J, Zhang HG. Mechanisms of Transition from Normal to Reentrant Electrical Activity in a Model of Rabbit Atrial Tissue: Interaction of Tissue Heterogeneity and Anisotropy. Biophys J. 2009 Feb 4;96(3):798-817.

[7] Yamashita T, Inoue H, Nozaki A, Sugimoto T. Role of anatomic architecture in sustained atrial reentry and double potentials. Am Heart J. 1992 Oct;124(4):938-46.

[8] Yamabe H, Misumi I, Fukushima H, Ueno K, Kimura Y, Hokamura Y. Conduction properties of the crista terminalis and its influence on the right atrial activation sequence in patients with typical atrial flutter. Pacing Clin Electrophysiol. 2002 Feb;25(2):132-41.

[9] Kuo SR, Trayanova NA. Action potential morphology heterogeneity in the atrium and its effect on atrial reentry: a two-dimensional and quasi-three-dimensional study. Philos Transact A Math Phys Eng Sci. 2006 Jun 15;364(1843):1349-66.

[10] Jalife J, Gray RA, Morley GE, Davidenko JM. Self-organization and the dynamical nature of ventricular fibrillation. Chaos. 1998 Mar;8(1):79-93.

[11] Clayton RH, Holden AV. Dynamics and interaction of filaments in a computational model of re-entrant ventricular fibrillation. Phys Med Biol. 2002 May 21;47(10):1777-92.

[12] Gray RA, Pertsov AM, Jalife J. Spatial and temporal organization during cardiac fibrillation. Nature. 1998 Mar 5;392(6671):75-8.

[13] Fenton F, Karma A. Vortex dynamics in three-dimensional continuous myocardium with fiber rotation: Filament instability and fibrillation. Chaos. 1998 Mar;8(1):20-47.

[14] Iyer AN, Gray RA. An experimentalist's approach to accurate localization of phase singularities during reentry. Ann Biomed Eng. 2001 Jan;29(1):47-59.

[15] Zou R, Kneller J, Leon LJ, Nattel S. Development of a computer algorithm for the detection of phase singularities and initial application to analyze simulations of atrial fibrillation. Chaos. 2002 Sep;12(3):764-78.

[16] Puwal S, Roth BJ, Kruk S. Automating phase singularity localization in mathematical models of cardiac tissue dynamics. Math Med Biol. 2005 Dec;22(4):335-46.

[17] Zhang Y, Xia L, Gong YL, Chen LG, Hou GH, Tang M. Parallel solution in simulation of cardiac excitation anisotropic propagation. Lect Notes Comput Sc. 2007;4466:170-9.

[18] Seemann G, Hoper C, Sachse FB, Dossel O, Holden AV, Zhang HG. Heterogeneous three-dimensional anatomical and electrophysiological model of human atria. Philos T R Soc A. 2006 Jun 15;364(1843):1465-81.

[19] Bosch RF, Zeng X, Grammer JB, Popovic K, Mewis C, Kuhlkamp V. Ionic mechanisms of electrical remodeling in human atrial fibrillation. Cardiovasc Res. 1999 Oct;44(1):121-31.

[20] Bray MA, Wikswo JP. Use of topological charge to determine filament location and dynamics in a numerical model of scroll wave activity. Ieee T Bio-Med Eng. 2002 Oct;49(10):1086-93.

[21] Gray RA, Wikswo JP, Otani NF. Origin choice and petal loss in the flower garden of spiral wave tip trajectories. Chaos. 2009 Sep;19(3):033118.

Address for correspondence.

Ling Xia
Department of Biomedical Engineering, Zhejiang University, Hangzhou 310027, China
E-mail: xialing@zju.edu.cn